CONSIDERATIONS FOR STARTING COMBUSTION ENGINES WITH AC MACHINES

Mauricio MONROY , **Carlos A. ROMERO** , **Edison HENAO**

Universidad Tecnológica de Pereira, Colombia
*Corresponding author, e-mail: mauriciomonroy@utp.edu.co

Abstract

To initiate its combustion cycles, internal combustion engines require a minimum rotational speed that can be given from several sources (muscular, electrical, pneumatic, among others). Advantages of initiating an ICE with an AC electrical machine is that it can integrate starter motor and generator in one device, provide a linear ramp of acceleration when starting, and assist the ICE in torque production. This article illustrates considerations for the design of a starting system with an AC electrical machine. Initially, criteria of torque, rotational speed and power requirements are analysed, considering resistances of compression, friction, and inertia of the slider-crank mechanism, as well as accessories, with a preliminary experimental validation. Also, types of three-phase AC electrical machines are put to comparison, as well as their associated electronic components needed for driving them in each case, concluding that AC induction machines require a complex 4-quadrant inverter. PM synchronous machines require a simpler inverter, but with highly specified power electronics components. The classical wound rotor machine requires the simplest inverter, with unidirectional power flow, less power transfer losses and less critical power electronics components. Finally, considerations for using of a battery assisted with supercapacitor as complementary DC power source are made.

Keywords: internal combustion engine, starter motor, AC machine, torque requirements, ISG, supercapacitor.

List of Symbols/Acronyms

ICE – Internal Combustion engine;
AC – Alternating Current;
DC – Direct Current;
TDC – Top Dead Centre;
BDC - Bottom Dead Centre;
ISG – Integrated Starter Generator;
ESR – Equivalent Series Resistance;
SRM – Switched Reluctance Machine.
PM – Permanent magnet

1. INTRODUCTION

The ICE requires for its normal operation a crankshaft's rotational speed that allows the continuity of its combustion cycles. As the ICE by its principle of operation has no starting torque, an initial turning of the crankshaft is needed to achieve a minimum rotational speed of the ICE, beginning from its standstill condition. An additional challenge appears at cold starting where the engine's crankshaft resists more to be turned [1].

Along with the development of the ICE, muscular, cartridge, electric, pneumatic starting systems have been implemented. The muscular ones are present in variants of a cord wound into a spool, an elbow-like bent bar (crank) or a pedal. A disadvantage of the muscular methods consists on the risk of injury when moving the mechanism.

Among the variants of pneumatic starting systems, an independent pneumatic motor can be coupled to the ICE, or as second option, by means of distribution valves, an injection of compressed air is performed directly to the cylinders of the ICE, having in account the timing and position of every cylinder, making injections after TDC [2].

With the electric starting, an electrical machine provides a transient torque to the ICE to accelerate it, using an electric circuit, usually of direct starting kind (DC power source-DC electric motor-Switch), as shown in Dziubiński et al [3].

The present work shows considerations about starting an ICE by means of an AC machine, an electronic DC to AC inverter and a DC supply.

It´s advantageous to use an AC electrical machine as it can integrate generator and starter motor in one device (ISG), also it could boost the torque output of the ICE at some regimes, which could lead to a reduction of the displacement of the ICE, a tendency for production of engines shown by Gheorghiu [46] that aims to reduce contaminant emissions. For the case of the electrical generation, one of the usual accessories coupled to the ICE is the alternator, which is a synchronous three-phase electrical machine, whose electrical scheme is

shown in works like the ones of Bogariz [4] and Neacsu [13].

In the next paragraph of this work, the ICE is seen as the load to be driven by the electric machine, irrespective of its DC or AC type. Then, based on existent literature, requirements of starting torque and target angular rotational speed are shown, in order to attain in more detail the resistant torque terms from compression, inertia, friction, and accessories of the ICE.

To validate the calculations, a DC motor (3), a torque sensor (2) and an ICE (3), shown in figure 1, are connected, so the engine is motored to obtain actual values of starting torque.
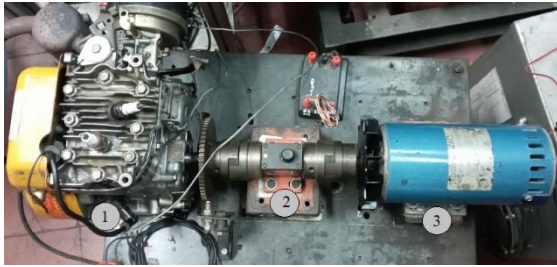

Fig. 1. Test bench

Once minimum values of starting torque and rotational speed are determined, the next paragraph will present a discussion of the type of AC machine with their associated electronic driver systems, considering that the electronic driver must be both a DC to AC inverter that provides alternating current to cause rotation of the electrical machine's axle and an AC to DC rectifier with regulation of the output back to to the battery and electrical accessories once the electrical machine becomes a generator and the ICE the propeller. After that, in the final paragraph, considerations of using supercapacitor and a battery as complementary DC power sources are made.

2. REQUIRED POWER AND TORQUE TO JUMPSTART AN ICE

The mechanical power P_m of a rotating motor is the product of the torque M at its shaft and its angular speed ω. From the work of Romero et al [5], the power needed for a DC starter motor is:

$$P_{st} = (54 + 365V_{mci})v^{0,53}n_{stm}^{1,35}\frac{\pi k}{\eta} \qquad (1)$$

Where: $V_{mci} = \pi\ i\ S\ D^2/4$ is the displacement of the ICE, with i cylinders, S the piston stroke and D its diameter. v is the kinematic viscosity of the lubricant, n_{stm} the minimum rotational speed that must be achieved so the ICE starts its self-sustained operation, k is the service factor and η is the mechanical efficiency of the transmission between the starter motor and the ICE.

In the document of Robert Bosch [6] about starting systems, a selection chart is presented with certain references of starter motors, as a function of the displacement of the ICE, both for spark-ignition and compression engines. However, the application

of the document is for DC starter motors, temporarily coupled to a reducing transmission bendix pinion-flywheel. The transmission ratio between those gears is typically between 9:1 to 11:1 [7, 8, 10, 11], for series-wound DC motors, or up to 90:1 for permanent-magnet stator DC motor and integrated planetary reduction gear [9].

From Eide [2] it can be stablished that the starting torque needed by unitary displacement volume is also a function of the number of cylinders, with special cases for a reduced number of cylinders. In Table 1, values of starting torque per litre of displacement as a function of the number of cylinders are presented. Note that the values of Table 1 are related to the torque at the output shaft of a DC series-wound motor, coupled with a bendix-flywheel reduction to the ICE. Those values are explained because, the more the cylinders, the less the non-regularity of output torque of the ICE, per Kett [12].

Table 1. Starting torque per litre of displacement as a function of the number of cylinders. After Denton [11]

i (cylinders)	M_{mst} / V_{mci} [N•m / l]
2	12,5
4	8,0
6	6,5
8	6,0
12	5,5

Also, there is information on Robert Bosch [6] and Neacsu [13] about the minimum flywheel cranking speed n_{stm}, which ranges between 60 min^{-1} and 90 min^{-1} for spark-ignition engines, 100 min^{-1} to 200 min^{-1} for compression-ignition engines and 150 min^{-1} to 180 min^{-1} for Wankel engines, given at a minimum temperature of typically 253 K.

For DC starter motors, these electrical machines must provide a nominal torque M_2 that helps maintain cranking speed n_{stm} for enough time to guarantee the self-sustaining combustion and a locked-rotor torque between 3 to 4 times M_2 to overcome static friction of the ICE [11].

On the other hand, Hutcheon [14] recommends in his work, as an empirical approximation, that M_{stm} at the crankshaft must be at least twice the specification of maximum torque output given by the ICE.

Although the previous information can provide an initial approximation, it is possible to review in more detail other relevant parameters of starting torque. The works of Patil and Ranade [7], Averbukh et al [15], DeBruin [16], Hutcheon and Marks [14], Dziubiński et al [3], Marchuk et al [17], allow to establish an equation that can be generalized:

$$M_{stm} = M_{gas} + M_{fric} + M_{acc} + M_L + M_{aa} \quad (2)$$

Where M_{stm} is the starting torque of the electrical machine at the ICE's crankshaft, M_{gas} the torque needed for gas compression (the engine in this case works as a compressor), M_{fric} the friction torque of the alternative mechanisms of the engine, including the gas distribution mechanism, M_{acc} the accessories'

DIAGNOSTYKA, Vol. 24, No. 1 (2023)
Monroy M, Romero CA, Henao E.: *Considerations for starting combustion engines with AC machines*

3

torque due to alternator, water pump, oil pump. M_L the load torque, M_{aa} the inertial torque of the components of the engine. The internal variables and parameters of the starting machine are not considered.

Figure 2 shows a generalized representation of the slider-crank mechanism, where ϕ corresponds to the crank angle, with respect to top dead centre (TDC). The value a is the distance of the cylinder axis with respect to the crankshaft axis. L is the length of the connecting rod.
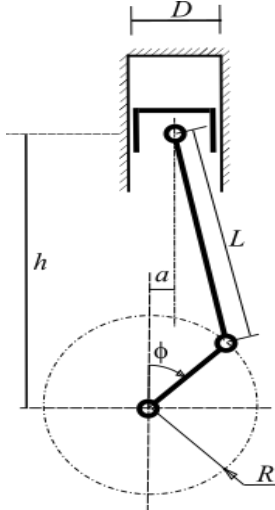

Fig. 2. Slider-crank mechanism

With stroke S, given in the specifications of the engine, and with centered mechanism ($a = 0$), the crank length is $R = 0,5\ S$. The ratios between crank length and connecting rod length λ_m and displacement ratio k_m are:

$$\lambda_m = \frac{R}{L} \qquad \text{and} \qquad k_m = \frac{a}{R}$$

From work of Romero [18]: $0{,}24 \le \lambda_m \le 0{,}31$, and $0{,}05 \le k_m \le 0{,}15$.

The piston displacement S_p is a function of the crank angle and dimensions of the mechanism:

$$S_p = R((1 - \cos(\phi)) + \frac{\lambda_m}{4}(1 - \cos(2\phi)) - k_m\lambda_m \sin(\phi)) \qquad (5)$$

Derivating the previous equation with respect of time, the piston velocity v_p is:

$$v_p = R(\sin(\phi) + \frac{\lambda_m}{2}\sin(2\phi) - k_m\lambda_m \cos(\phi))\frac{d\phi}{dt} \qquad (6)$$

Derivating equation (6), the piston acceleration A_p is:

$$A_p = R(\cos(\phi) + \lambda_m \cos(2\phi) + k_m\lambda_m \sin(\phi))\frac{d^2\phi}{dt^2} \qquad (7)$$

Now, from Armas [19], the instantaneous cylinder volume V, considering the linear deformations of the linkages, can be obtained as follows:

$$V = V_{cc} + \Delta V_p + \Delta V_i + V_h = V_{cc} + \frac{\pi D^2}{4}(\Delta L_p + \Delta L_i + s_p) \qquad (8)$$

Where: D is the diameter of the cylinder, V_{cc} the volume of the combustion chamber at TDC, ΔV_p is the change in volume due to the deformation of the mechanism, caused by the gas pressure. ΔV_i is the change in volume due to deformation caused by inertia and V_h is the instantaneous geometric volume as a function of the crank angle.

As the volumes are cylinders, they can be expressed as lengths times the area, so the lengths are:

$$L_{cc} = \frac{S}{\varepsilon - 1} \qquad (9)$$

$$\Delta L_p = \frac{2K_{def}}{E}\left(\frac{D}{d_{Bul}}\right)^2 (h_c + L + \frac{S}{2})p \qquad (10)$$

$$\Delta L_i = \frac{4K_{def}m_j}{\pi d_{bul}^2 E}(h_c + L + \frac{S}{2})A_p \qquad (11)$$

Where: ε is the compression ratio, K_{def} is the deformation coefficient of the ICE, E is the Young modulus of the connecting rod, d_{Bul} is the diameter of the piston pin, m_j is the mass that participates in the reciprocating motion, h_c is the height of the head of the piston from the axis of the gudgeon pin and p is the gas pressure. Assuming a flat cylinder head, $V_{cc} = \pi D^2 L_{cc} / 4$.
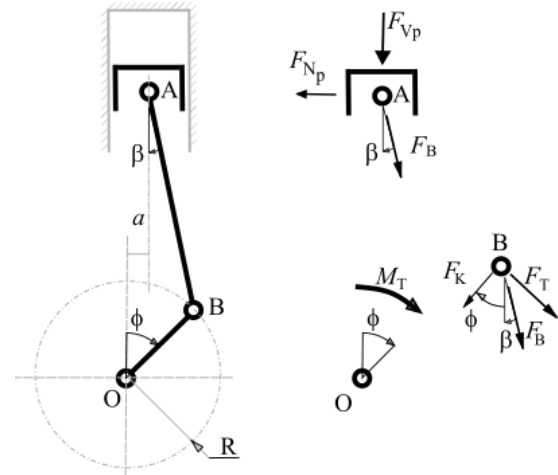

Fig. 3. Forces at the slider-crank mechanism

Figure 3 shows some of the forces of the mechanism at the linkages, and torque M_T at the crank.

The relations between forces and dimensions of the mechanism are:

$$F_B = \frac{1}{\cos(\beta)}F_{Vp} \qquad (12)$$

$$F_{Np} = \tan(\beta) . F_{Vp} \qquad (13)$$

$$F_T = \sin(\phi + \beta) F_B = \frac{\sin(\phi + \beta)}{\cos(\beta)}F_{Vp} \qquad (14)$$

$$F_K = \cos(\phi + \beta) F_B = \frac{\cos(\phi + \beta)}{\cos(\beta)}F_{Vp} \qquad (15)$$

$$\beta = \arcsin(\lambda_m \sin(\phi) - k_m \lambda_m) \qquad (16)$$

$$M_T = R . F_T \qquad (17)$$

F_{Vp} corresponds to the reciprocating force on the piston and can be expressed as a function of the absolute pressure of the chamber as follows:

$$F_{Vp} = \frac{\pi}{4}D^2(p - p_0) \qquad (18)$$

From the instantaneous volume, pressure at combustion chamber p in motored condition is determined considering polytropic compression as:

$$\frac{p}{p_{CA}} = \left(\frac{V_{CA}}{V}\right)^n \tag{19}$$

p_o is the absolute crankcase pressure, p_{CA} is the pressure when closing the intake valve, V_{CA} its volume and $n = 1,35$ the mean motored polytropic exponent [19].

The gas compression torque term is, as a function of gas pressure and crank angle:

$$M_{gas} = \frac{\pi}{4} R . D^2 \frac{\sin(\phi+\beta)}{\cos(\beta)} (p - p_0). \tag{20}$$

When starting the ICE, as combustion hasn't begun yet, the maximum normalized contribution of change in volume due to compression is $\Delta V_p / V = 0,001$ at TDC. And as the process begins from standstill, ΔV_i can be also disregarded.

The inertia term M_{aa} contributes to the reciprocating force on the piston as follows:

$$F_{Vpj} = m_j A_p = -m_j R(\cos(\phi) +$$
$$\lambda_m \cos(2\phi) + k_m \lambda_m \sin(\phi))\frac{d^2\phi}{dt^2} \tag{21}$$

$$m_j = m_{pis} + m_{bul} + \kappa_b m_b \tag{22}$$

The inertial contribution of the piston to M_{aa} is:

$$M_{TV} = -m_j R^2 . \frac{\sin(\phi+\beta)}{\cos(\beta)} (\cos(\phi) +$$
$$\lambda_m \cos(2\phi) + k_m \lambda_m \sin(\phi))\frac{d^2\phi}{dt^2}. \tag{23}$$

The inertial contribution of connecting rod is:

$$M_{Tb} = -(1 - \kappa_b) m_b R^2 . \frac{d^2\phi}{dt^2} \tag{24}$$

The rotational inertial contribution of crankshaft is:

$$M_{TCk} = -(m_m R^2 + J_{mp}) . \frac{d^2\phi}{dt^2} \tag{25}$$

$$m_m = m_{mb} + \frac{2}{R} \rho_m m_c \tag{26}$$

The inertial torque to overcome is then:

$$M_{aa} = M_{TV} + M_{Tb} + M_{tCk} \tag{27}$$

Where m_{pis} is the piston mass, m_{bul} gudgeon pin and sleeve bearing masses, κ_b the fraction of the connecting rod that participates in the linear motion where $0,25 \le \kappa_b \le 0,275$ per Romero [18] and m_b connecting rod mass. m_m is the total mass of crankshaft elements, m_{mb} mass of crankpin journals, m_c counterweights' mass, ρ_m distance between crankshaft axis and center of gravity of counterweights and J_{mp} mass moment of inertia of main journals. Also, the mass moment of inertia of the flywheel must be included.

The time of the starting process t_{st} and the target cranking speed n_{stm} provide the value of the angular acceleration as follows:

$$\frac{d^2\phi}{dt^2} = \frac{\pi n_{stm}}{30 t_{st}} \tag{28}$$

That because, unlike the DC direct-connected starter motors, with an electronic variable frequency drive and an AC machine it is possible to set a constant acceleration ramp from standstill to the target cranking speed.

The friction term M_{fric} appears as an equivalent force on the piston:

$$F_{Vpf} = \frac{\pi}{4} D^2 (p_f) \tag{29}$$

For Ferguson [20], it's not simple to obtain an expression for the equivalent indicated pressure friction loss p_f. The relationship between friction force F_f and normal force F_n is given by the friction coefficient, described by the Stribeck friction regime diagram, shown in figure 4, which relates c_f with the Stribeck number SV.

$$c_f = \frac{F_f}{F_n} = \frac{\tau}{\sigma_n} \tag{30}$$

The Stribeck number relates the relative velocity between surfaces, viscosity and normal stress.

For surfaces with rotational motion between them:

$$SV = \frac{\mu}{\sigma_n} \omega_{rel} \tag{31}$$

For surfaces with linear motion between them:

$$SV = \frac{\mu L_{con}}{F_n} U_{rel} \tag{32}$$

With: μ dynamic viscosity, σ_n the specific stress, L_{con} the contact length between surfaces, ω_{rel} and U_{rel} the relative angular and linear velocities between surfaces respectively.

There are three lubrication regimes shown in the Stribeck diagram of figure 4: limit (1), mixed (2) and hydrodynamic (3). In the hydrodynamic regime, the relative velocity and viscosity of lubricant create a pressure that supports the surfaces avoiding its contact, and c_f becomes directly proportional to velocity. In the mixed regime, c_f increases and there is intermittent metal-to-metal contact. In the limit regime, there is mostly metal-to-metal contact and c_f is a maximum.
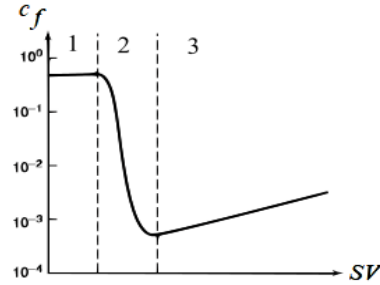

Fig. 4. Stribeck diagram. After Ferguson [20]

When starting an ICE, the initial displacements occur at limit regime. Once the crankshaft gains speed, the crank journals' friction passes to hydrodynamic regime. For the piston and its rings, their friction against the cylinder have limit regime when piston is at TDC and BDC, but at the middle of the stroke, where piston velocity is maximum, the regime can be hydrodynamic [20].

The friction analysis presented in Ferguson [20] indicates that the most friction contribution is present at piston, rings and cylinder with 50% to 75% of the total friction loss of the engine.

The work of Kamil et al. [21] proposes expressions for the equivalent pressure loss p_f due to crankshaft journals p_{Fcrank}, piston-cylinder p_{Frecip}, valvetrain $p_{Ftrvalv}$, pumping losses p_{Fbom} and accessories' loss p_{Facc}.

$$p_f = p_{Fcrank} + p_{Frecip} + p_{Ftrvalv} + p_{Fbom} + p_{Facc} \tag{33}$$

Where the terms depend on the viscosity of the oil, the crankshaft speed, journals diameter, journal length, number of journals, mean piston velocity, constants that depend on the configuration of the valvetrain, number of valves, maximum valve lift, atmospheric pressure, intake manifold pressure, ratio of intake valve diameter and cylinder, ratio exhaust valve diameter – cylinder diameter.

From the model of Kamil et al. [21], the percentages of p_f for each contribution are: $p_{Fcrank} = 11,4\%$, $p_{Frecip} = 40,9\%$, $p_{Ftrvalv} = 18,5\%$, $p_{Fbom} = 14,7\%$ and accessories' loss $p_{Facc} = 14,5\%$ respectively.

The friction torque to overcome, including accessories, is then:

$$M_{fric} + M_{acc} = \frac{\pi}{4} R . D^2 \frac{\sin(\phi+\beta)}{\cos(\beta)} (p_f - p_0) . (38)$$

Considering all the previous information, a preliminary estimation for the required starting torque at the crankshaft and power of the electric starter motor of a Robin EY-15 engine was made. The parameters of the engine are: Displacement = 143cm^3; D = 63mm; S = 46mm; L = 96mm; ε = 8,5.

Table 2 shows the results of the criteria of equation (1) after Romero [5] with 10W40 oil of density 830kg/m^3 and viscosity 116cSt@313K [42]; k=1,5;η=0,9. Next row from table 1 after Denton [11], assumes 16 N•m/l by extrapolation at 253K which gives an electric motor torque of 2,3 N•m and adding a reduction with gear ratio of 10:1, since the criterion is applicable for bendix-flywheel transmission. Third row from Hutcheon [14] comes from using twice the engine's maximum torque [41] and the last row is the application of the formulas (2) to (28) of this work.

After coding the expressions (2) to (20) into a mathematical model and using the parameters of the EY-15, the results of such model are shown in figure 5, where compression torque M_{gas} is the blue curve and pressure p is the orange one.

As the EY-15 is a 4-stroke engine with one cylinder, one cycle requires 720 degrees of crank rotation. The intake stroke corresponds to the interval $0°<\varphi<180°$, i.e. from TDC to BDC, not shown in figure 5. The next and most relevant crank angle interval is $180°<\varphi<360°$ and corresponds to the turning force needed to compress the air-fuel mixture moving piston from BDC to TDC. As shown in figure 5, the worst case of gas compression braking torque M_{gas}, occurs approximately at φ=336°, that the starter motor must overcome. The point of maximum pressure p = 9,2 bar occurs at φ=360°.

Having a peak of 17 N•m for the compression term, the formulas (21) to (28) add 0,3 N•m of maximum contribution due to mass moment of inertia of parts of the engine including flywheel, and a linear acceleration from 0 to 200 min^{-1} in 4 seconds. For the case of friction torque term, it is assumed 20% more than the sum of the previous results. That additional 20% comes from the

considerations of Ferguson [20] after Gish, where the contribution in pressure to friction is around 1 bar to 1,5 bar. Finally, target cranking speed was n_{stm} = 200min^{-1}.
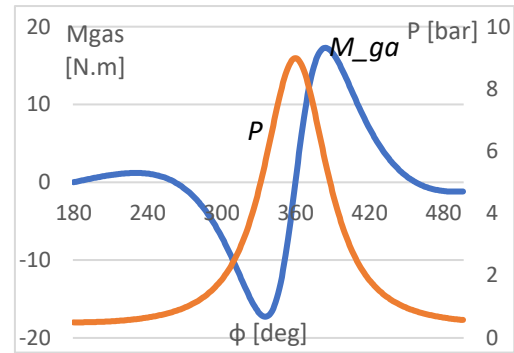

Fig. 5. Motored torque and gas pressure

Table 2. Estimated starting torque

Consideration	M_{mst} [N•m]	Power [W]
Romero	17,1	357
Denton	23,0	480
Hutcheon	13,4	281
Simulation	20,6	428

For preliminary verification of calculations, a DC permanent-magnet motor, with a power of 750W at 1750 min^{-1} and a nominal torque of 6,1N•m [44] was coupled to a Futek torque sensor and this one to an EY-15 engine, as shown previously in figure 1. As this DC motor has 3 times that nominal torque in locked-rotor condition, it could successfully jumpstart the engine at an ambient temperature of 298K. Once the setup of figure 1 was made, starting torque (blue curve) and angular speed (orange curve) data obtained from the Futek sensor are shown in figure 6. The EY-15 engine required a first peak of 11,23 N•m at the beginning, then a second peak of 9,37 N•m and successive peaks of 5 N•m each time there was compression. That 5 N•m value is justified as that the engine has signs of wear due to many hours of testing. Rotational speed achieved was 555 min^{-1} (orange curve). This test was made with 24V, 7Ah lead-acid battery directly connected to the motor, below its 90V DC supply specification, hence the deceleration at 0,25s.

3. SELECTION OF THE AC STARTING MACHINE

From the estimation of starting torque, a speed reducing transmission between ICE and starter motor could be needed.

The transmission will connect both machines permanently, thus making the electric machine an *Integrated Starter and Generator* unit (ISG). If the AC machine is connected directly to ICE's crankshaft, as shown in Viorel et al. [22], both machines will have the same rotational speed, but the starter mode of the AC machine is needed only from standstill to the target cranking speed.
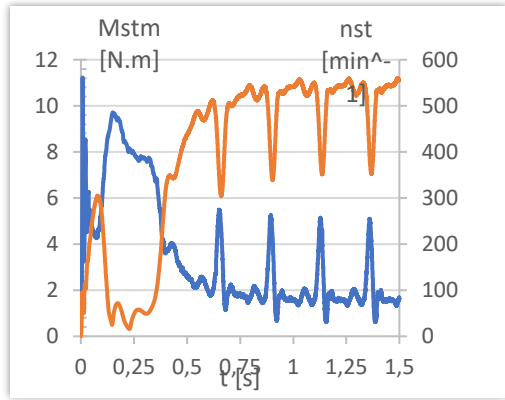
Fig. 6. Starting torque and rotational frequency

If the product of torque by rotational speed leads to high requirements of the AC machine, a transmission is preferred.

In this case the transmission ratio is:

$$u = \frac{n_{stm}}{n_{ICE}} \qquad (39)$$

And the required torque is:

$$M_{stm} = \frac{M_{ICE}}{\eta \cdot u} \qquad (40)$$

Where: n_{stm} and n_{ICE} are the rotational speeds of the AC machine and ICE respectively, η is the efficiency of the transmission, M_{ICE} and M_{stm} are the torques received by ICE and the one provided by the AC machine respectively.

In Henry et al. [23] a 3 to 1 reducing transmission with a toothed belt is used, where the AC machine pulls up to 1200 min^{-1}, providing a starting ICE speed of 400 min^{-1}.

The types of electrical machines that can be analyzed are the induction machine, the synchronous motor with wound rotor, permanent magnet rotor, axial or radial flux, and switched reluctance. All of them with three-phase supply, as they have a better power to weight ratio respect to a single-phase machine and no requirement of capacitors for starting [24].

3.1. Considerations for using an Induction Machine or Switched Reluctance Machine

From Chapman [24], when the induction machine is motored, it cannot provide reactive power, so the stator must be energized to maintain its own magnetic field. In Chapman [24] and Shuker [25] an induction machine and an external circuit with capacitors in delta configuration is shown, so the induction machine becomes an isolated generator. Using the residual magnetism of the rotor, the capacitors charge progressively. The rotor must rotate 2% to 5% above synchronous speed to maintain voltage generation [26]. In Henry et al. [23] and Grachev et al [27] a 42V field-oriented three-phase inverter is used. From those authors, an inverter scheme for ISG can be seen in figure 7.

The power supply is the battery U_B and the inverter is INV1, with 4-quadrant control.

In generator mode, INV1 feeds the stator from the battery to maintain generation, regulates the voltage to the battery as the rotational speed increases, and must avoid the direct polarization of the intrinsic diodes D1 to D6 [40]. The sensing signal of the rotational speed and slip is sent to the controller by terminals Tc1 and Tc2. In starter motor mode, INV1 provides switching to transistors Q1 to Q6, to feed variable frequency and voltage from U_B to the induction machine.
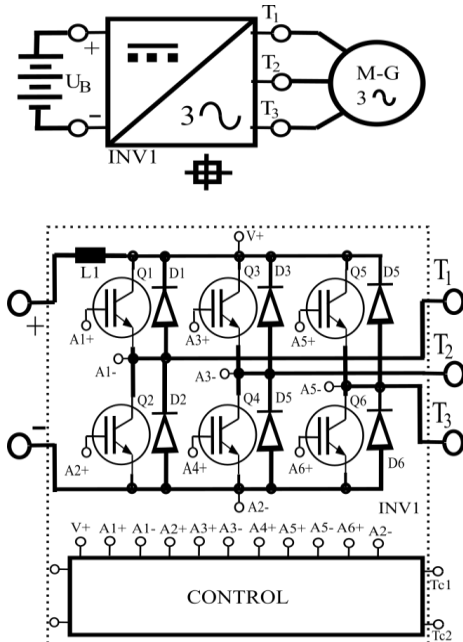

Fig. 7. Basic scheme for 4-Quadrant inverter for induction machine as ISG

For the switched reluctance machine (SRM), the scheme of the inverter is the same of the figure 7, although the generation and motoring depends on a sequence of activation of coils of the stator. A disadvantage of the SRM is the torque ripple, noise and vibrations [13, 23].

3.2. Considerations for using a permanent magnet (PM) synchronous machine

Both authors [23, 27] comment that a synchronous machine is more efficient than an induction one due to better torque-to-mass ratio and more convenient as the stator doesn't need to be energized to generate. In particular, the axial flux PM synchronous machine has more torque-to-mass ratio [28, 29].

Figure 8 shows the basic scheme for the inverter and regulator for a PM synchronous machine. Those electrical machines do not need brushes and slip rings [28, 29, 30], but in generator mode they require a DC-DC buck regulator (DCDC1) after the 3-phase rectification provided by the intrinsic diodes of the transistors Q1 to Q6 of INV2, all of them switched off in generator stage [13] (see figure 8).

The voltage of every stator coil is:

$$E_{ph} = k_g \omega \cos{(\omega t + \psi)} \qquad (41)$$

With ψ the phase of each coil, 0, $2\pi/3$ and $4\pi/3$ respectively.

As the ICE turns the synchronous machine, its angular speed ω, one of the factors that determine the

magnitude of the phase voltage, varies. Thus, the DC rectified voltage U_G of INV2 varies with rotational speed. The DC-DC regulator maintains the charging voltage for U_B.
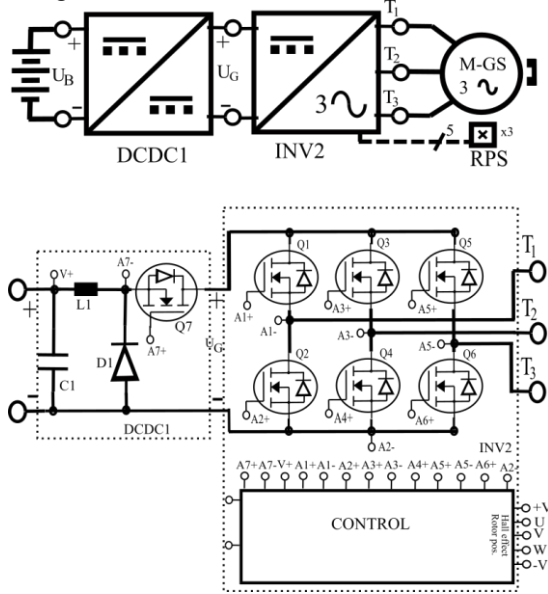

Fig. 8. Basic scheme for inverter and regulator for PM synchronous machine as ISG

The factor k_g is relatively constant, as well as the permanent magnet of the rotor of the synchronous machine holds its magnetic flux density. However, as explained in Calin and Helerea [34], that magnetic flux density can be affected by the temperature of the magnets.

In starter motor mode, Q7 of DCDC1 switches on saturated and connects the battery with the inverter INV2, so $U_G = U_B$. Then, INV2 switches transistors Q1 to Q6, to provide variable frequency and voltage to the synchronous machine. It is recommended the use of a detection of the position of the rotor (RPS) to provide the appropriate switching of Q1 to Q6 and to get better starting torque [34].

3.3. Considerations for using a wound rotor (WR) synchronous machine

The use of WR synchronous machines is common in automotive alternators, as shown in Blaga et al. [31]. Slip rings and brushes are required, but the stator voltage output can be controlled by changing the k_g term, and this in turn by means of modifying the rotor current i_{rot}:

$$k_g = k_{cons} i_{rot} = \frac{k_{cons}}{R_{rotor}} U_r \qquad (42)$$

The current i_{rot} can be varied along with the rotor voltage supply U_r. k_{cons} is the constructive constant of the AC machine and R_{rotor} the resistance of that moving winding.

The rotor voltage U_r is varied with the DC-DC buck regulator DCDC2, shown in figure 9.

The inverter INV2 is the connection between the stator and the battery.

In generator mode, Q1 to Q6 are inactive, working as intrinsic diodes for rectification, as

explained before in 3.2. The charging voltage to the battery U_B can be regulated by controlled variation of U_r from DCDC2. And in motor mode, Q7 of DCDC2 is switched on saturated, Q1 to Q6 are switched to provide variable frequency and voltage to the stator as explained earlier.

Although the scheme for induction machine of figure 7 appears to be simpler, the control strategy is more complex. In the scheme for PM synchronous machine of figure 8, Q1 to Q7 must be specified to withstand the currents of the stator, both in generator and motor mode. Also, the energy flow must be bidirectional. Respect to the scheme of 3.1, INV2 is simpler than INV1 as Q1 to Q6 can operate by default as rectifiers. For the scheme for WR synchronous machine, Q1 to Q6 must be specified to withstand stator currents, but Q7 is specified to withstand rotor current, which is less than stators [13]. DCDC2 is simpler than DCDC1, with unidirectional energy flow and with less current specifications.

4. CONSIDERATIONS FOR THE POWER SUPPLY

The power supply, when the AC machine acts as motor, must provide the required voltage and current. For batteries, as the energy is stored within a chemical reaction, its internal resistance depends on temperature. Curves of internal resistance with respect of temperature, for lithium-ion and lead-acid appear in the work of Lebkowski [35]. At lower ambient temperatures, the internal resistance of the battery increases, e.g, from 190mΩ at 293K to 290mΩ at 253K for 4AH lead-acid units. That can affect the electrical power delivery.

Supercapacitors have a very low internal equivalent series resistance (ESR), e.g. 7mΩ for a 48V, 171F unit [36]. Furukawa [37] shows that the ESR is 1mΩ at 293K and 2,6mΩ at 253K for a 400F unit. Thus, supercapacitors can deliver more transient current and higher voltage than batteries. However, supercapacitors have less energy density, around 0,8 W•h/kg to 10 W•h/kg [38], whereas lead-acid batteries carry a density around 35 W•h/kg to 50 W•h/kg, and lithium-ion between 90 W•h/kg and 120 W•h/kg [35]. The combination of both in parallel can deliver high transient power and store a good amount of electrical energy.

To calculate the capacitance and voltage of a supercapacitor module, the work of Rafik [39] refers an algorithm based on the energy delivered during jumpstart.

The energy delivered is:

$$\Delta W = P_{st} \Delta t = 0.5 C_{Wmoy} \left(\left(V_{max} - R_T I_{moy} \right)^2 - \left(V_{min} - R_T I_{moy} \right)^2 \right) \qquad (43)$$

Where P_{st} is the electrical power delivered during the starting time Δt, C_{Wmoy} is the mean capacitance, V_{max} is the maximum voltage at which the supercapacitor is charged, V_{min} is its minimum voltage, half of V_{max},
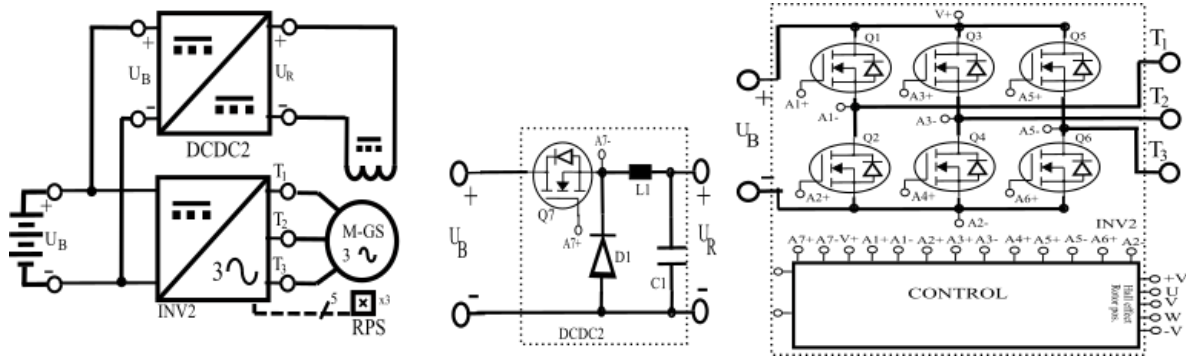
Fig. 9. Basic scheme for inverter and regulator for a wound-rotor synchronous machine as ISG

R_T is the ESR of supercapacitor, I_{moy} is the mean current supply in starting.

Figure 10 shows the connection between battery and supercapacitor, using a DC-DC converter DCDC3, which limits the current, having in account that both sources cannot be connected directly in parallel.
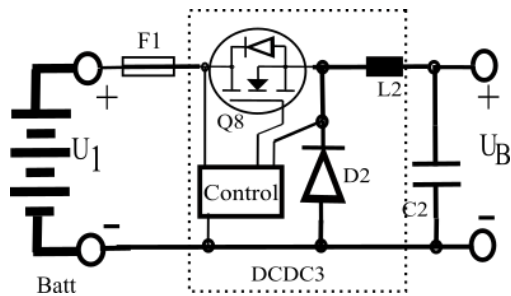

Fig. 10. connection of battery and supercapacitor. After Rafik [39]

5. CONCLUSIONS

Comparing criteria with the experimental test shown in figure 6, the formula seen in Romero [5] provides an estimation based on displacement of the ICE and viscosity of oil, this property highly dependent on temperature, so this formula provides the possibility to predict starting at different temperature conditions. The criteria shown in Denton [11], extrapolating for the single cylinder engine case, provided the highest estimation of torque. The criterion of Hutcheon [14] provided the lowest estimation. Although all mentioned criteria provided a greater value than the experimental one, the lowest estimation could lead to difficulties of starting in cold weather condition.

The analysis of forces and torques on the slider-crank mechanism provided a value between criteria seen in Romero and Denton, also greater than the experimental one, making it applicable, although the complete parameterization for the analysis was not possible. For this analysis, the compression torque is the greatest contributor to the resistance to starting, around 85%, having in account an ideal case where there are no compression losses. This analysis can be further improved from measurement of parameters that conform friction torque.

As the formulas of Romero, Denton and Hutcheon are for DC motors, and three-phase AC electrical machines have a locked-rotor torque between 2 and 3 times the nominal torque, a similar case found in DC machines, an ICE can be started also with an AC machine, with the advantage that the same electrical machine can operate as alternator. Also, the AC machine could assist the ICE not only at starting but in usual combustion regimes, adding torque output to it (hybrid powertrains), which in turn leads to require less displacement of the engine and to reduce contaminant emissions.

The type of AC machine leads to different requirements of electronic inverters and regulators, powered by DC power supply. Contrary to common knowledge, it is possible to use an induction machine as ISG, although it requires a 4-quadrant inverter with a complex control strategy that must maintain the magnetization of stator and its generation at the same time. The scheme for PM synchronous machine has a simpler control strategy in generation mode than the one for induction machine, although there are power electronics components with high specifications, having up to three transistors in series between power source and AC machine, which increases electrical power transfer losses. The scheme for WR synchronous machine requires the simplest case of inverter in generation mode and DC-DC regulators with unidirectional energy flow and less current specifications. Between power source and AC machine, there will be up to 2 transistors in series, which means less power transfer losses than PM synchronous drivers. For the case of starting, the mentioned machines require a very similar DC to AC three-phase conversion, except that for synchronous machines, a detection of position of rotor is desirable for better starting torque. Another potential advantage of using an AC machine is to provide a linear acceleration ramp when starting the ICE, contributing to less use of electrical power for that event.

The use of supercapacitor and battery allows more transient current and higher DC power source voltage that leads to a more reliable starting of the ICE, especially at low ambient temperatures.

Author contributions: *research concept and design, M.M., C.A.R., E.J.H.; Collection and/or assembly of data, M.M. C.A.R., E.J.H.; Data analysis and interpretation, M.M., E.J.H.; Writing the article, M.M., C.A.R., E.J.H.; Critical revision of the article, C.A.R., E.J.H.; Final approval of the article, C.A.R..*

Declaration of competing interest: *The authors declare that they have no known competing financial interests or personal relationships that could have appeared to influence the work reported in this paper.*

REFERENCES

1. Barthe M. Rotative Engines. Typologies and alternative fuels. Motores rotativos. Tipologías y combustibles alternativos. Proyecto de final de carrera. Facultat de Náutica de Barcelona -UPC. 2009.
2. Eide TI. Modelling and control of a pneumatic starting system for medium-speed gas engines. Norwegian University of Science and Technology. Department of Marine Technology. 2011. https://core.ac.uk/download/pdf/30857651.pdf.
3. Dziubiński M, Drozd A, Kordos P, Syta A. Diagnosing the automobile starting system. Combustion Engines. 2017;170(3):19-23. https://doi.org/10.19206/CE-2017-303.
4. Bogariz D. (Experimental validation of a three-phase alternator model (40V) for automotive application). Validación experimental de un modelo de alternador trifásico (40v) para automoción. Universitat Rovira I Virgili. Escuela Técnica Superior de Ingeniería. Departamento de ingeniería Electrónica Eléctrica y Automática. 2003.
5. Romero CA, Rodríguez A, Monroy M. (Assembly and instrumentation of a didactic test bench for testing of starting of internal combustion engines). Ensamble e instrumentación de un banco didáctico para pruebas de arranque en motores de combustión interna. Revista UISIngenierías. 2020;19(3):37-48. https://doi.org/10.18273/revuin.v19n3-2020004.
6. Robert Bosch GmbH. Starting systems. In: Robert Bosch GmbH (eds) Bosch Automotive Electrics and Automotive Electronics. Bosch Professional Automotive Information. Springer Vieweg, Wiesbaden. 2014. https://doi.org/10.1007/978-3-658-01784-2_17.
7. Patil AB, Ranade NS. Computer Simulation of an I.C. Engine During Cranking by a Starter Motor. SAE Technical paper series. 1993:930626.
8. Bonnick A, Newbold D. A practical approach to motor vehicle engineering and maintenance. 3rd. Ed. Taylor and Francis Group. 2017.
9. Ma Q, Rajagopalan SSV, Yurkovich S, Guezennec Y. A High-Fidelity Starter Model for Engine Start Simulations. Proceedings of the American Control Conference. 2005.
10. Laughton MA, Warne DA. Electrical Engineer's Reference Book. Sixteenth Edition. Newnes. 2003.
11. Denton T. Automobile Electrical and Electronic Systems. 5th. Ed. Abingdon-on-Thames: Routledge. 2017.
12. Kett PW. Motor Vehicle Science Part 2. Variable torque, force and work done (C8). Springer, Dordrecht. 1982. https://doi.org/10.1007/978-94-009-5943-9_8.
13. Neacşu DO. Automotive Power Systems. CRC Press. 2020.
14. Hutcheon KF, Marks RL. Developments in starter motor application to diesel engines. Proc. Instn. Mech. Engrs. 1969-70. Vol. 184 Pr. 3A. Paper 13. Univ of Cincinnati.
15. Averbukh M, Rivin B, Vinogradov J. On-Board Battery Condition Diagnostics Based on Mathematical Modeling of an Engine Starting System. SAE Technical paper series. 2007-01-1476. 2007 World Congress Detroit, Michigan April 16-19, 2007.
16. DeBruin LA. Energy and Feasibility Analysis of Gasoline Engine Start/Stop Technology. The Ohio State University. 2013.
17. Marchuk A. Kuharenok G. Petruchenko A. Successfull diesel cold start through proper pilot injection parameters selection. Robert Bosch Company. Belarussian National Technical University.
18. Romero CA. (Fundamentals of construction and calculation of internal combustion machines). Fundamentos de construcción y cálculos de máquinas de combustión interna. Universidad Tecnológica de Pereira. 2002.
19. Armas O. (Experimental Diagnostic of the combustion process in direct injection diesel engines). Diagnóstico experimental del proceso de combustión en motores diésel de inyección directa. Departamento de Máquinas y motores térmicos. Universidad Politécnica de Valencia. SPUPV-98.2207.
20. Ferguson C, Kirkpatrick A. Internal combustion engines. Applied thermosciences. 3rd edition. Wiley. 2016.
21. Kamil M, Rahman MM, Bakar RA. An integrated model for predicting engine friction losses in internal combustion engines. International Journal of Automotive and Mechanical Engineering (IJAME). 2013:P176,
22. Viorel IA, Szabó L, Löwenstein L, Ştet C. Integrated starter-generators for automotive application. Acta Electrotehnica. 2004;45(3).
23. Henry R, Lequesne B, Chen S, Ronning J. Belt-Driven Starter-Generator for Future 42-Volt Systems. SAE Technical Paper 2001-01-0728, 2001, https://doi.org/10.4271/2001-01-0728.
24. Chapman SJ. Electric Machinery fundamentals. McGraw-Hill. 2012.
25. Shuker ZS. Three-phase induction motor conversion to three-phase induction generator. Journal of Engineering and Development. 2015;19(5).
26. Marathon Electric Generators. Primeline Induction Generator. www.marathonelectric.com. 2012. Regal-Beloit Corporation. SB317.
27. Grachev PY, Strizhakova EV, Tabachinskiy AS. Starter-Generator Design and Dynamic Processes Simulation for HEVs. International Conference on Industrial Engineering, ICIE 2017. Procedia Engineering. 206:1877-7058. https://doi.org/10.1016/j.proeng.2017.10.490.
28. Radwan-Pragłowska N, Wegiel T, Borkowski D. Modeling of axial flux permanent magnet generators. Energies. 2020;13:5741; https://doi.org/10.3390/en13215741.
29. Sadeghierad M, Darabi A. Lesani H, Monsef H. Design Analysis of High-Speed Axial-Flux Generator. American J. of Engineering and App. Sci. 2008;1(4): 312-317.
30. Cathey JJ. Electric machines: Analysis and design applying MATLAB. McGraw-Hill. 2002.
31. Blága C, Szabó N. Simulation and measurement of a voltage regulator of an automotive generator.16th

International Power Electronics and Motion Control Conference and Exposition. Antaya. Turkey. 2014.

32. Enache BA, Constantinescu LM, Lefter E. Modeling aspects of an electric starter system for an internal combustion engine. ECAI 2014. International Conference. 5th. Ed. Electronics, Computers and Artificial Intelligence. 2014. Bucharest. Romania.

33. Simoes MG. Modeling a self-excited induction generator. Colorado School of Mines. Golden. Electrical Engineering Department. 2019. https://doi.org/10.25676/11124/173037.

34. Calin M, Helerea E. Temperature influence on magnetic characteristics of NdFeB permanent magnets. 2011 7th International symposium on advanced topics in electrical engineering (ATEE) IEEE. 2011.

35. Lebkowski A. Temperature, overcharge and short-circuit studies of batteries used in electric vehicles. Przeglad Elektrotechniczny. Gdynia Maritime University, Department of Ship Automation. 2017. https://doi.org/10.15199/48.2017.05.13.

36. Cultura AB, Zalameh ZM. Modeling, evaluation and Simulation of a supercapacitor module for energy storage application. Proceedings of the International conference on computer information systems and industrial applications (CISIA). 2015. https://doi.org/10.2991/cisia-15.2015.235.

37. Furukawa T. Capacitors for Internal Combustion Engine Starting with Green Technology DLCAP. EVS24 International Battery, Hybrid and Fuel Cell Electric Vehicle Symposium. World Electric Vehicle Journal. 2009;3(2):233-237. https://doi.org/10.3390/wevj3020233.

38. Kim S, Chou P. Energy harvesting with supercapacitor-based energy storage. In: Smart sensors and systems. Springer. 2015. https://doi.org/10.1007/978-3-319-14711-6_10.

39. Rafik F, Gualous H, Gallay R, Karmous M. A Berthon. Contribution to dimensioning a pack of supercapacitors for 12V/42V application. U.S. Department of Energy. Office of Scientific and Technical Information. 2004. https://www.osti.gov/etdeweb/servlets/purl/20823693

40. Dixon J. Three phase controlled rectifiers. department of electrical engineering. Pontificia Universidad Católica de Chile. 2007. https://doi.org/10.1016/B978-012088479-7/50030-4.

41. Subaru Industrial Products Co. Ltd. Engines EY series. https://www.subarupower-global.com/engines/ey-series/ey15-3d.

42. Subaru Industrial Products Co. Ltd. Engines EY series. Parts Manual. PUB-EP5657A Rev. 04/00. https://subarupower.com/media/manuals/1288973986 09319075.pdf.

43. Kumbir V, Dostil P. Cupera J. Sabaliauskas A. Kinematic viscosity of four-stroke engine oils. Mendel University in Brno. Siauliai University. Technologijos Mochslai Mechanine Inzinerija. 2012. Jaunųjų mokslininkų darbai. Šiauliai : VšĮ Šiaulių universiteto leidykla. 2012;3(36):134-139.

44. ABB Motors and Mechanical inc. Baldor Reliance. Product information packet. CDPWD3445. 1HP, 1750rpm, DC, 56C, 3435P, TEFC, F1.

45. Wierzbicki S. Diagnosing microprocessor controlled systems. Polska Akademia Nauk, Teka Komisji Motoryzacji i Energetyki Rolnictwa, Tom VI, Lublin, 2000: 183-188

46. Gheorghiu V. Atkinson cycle and very high-pressure turbocharging: increasing internal combustion engine efficiency and power while reducing emissions. Hamburg University of Applied Sciences, Berliner Tor 21, Hamburg Germany, 2016.

Mauricio MONROY received Ms.C. degree in Automated Systems of Production from Pereira Technological University, Pereira, Colombia, in 2005. Now he works at Pereira Technological University. His current research interests include Internal combustion machine, instrumentation, automation and electrical machines.

Carlos ROMERO received Ph.D. degree in Mechanical Engineering from Valencia Polytechnic University, Valencia, Spain, in 2009. Now he works at Pereira Technological University. His current research interests include internal combustion machine, and machine design.

Edison HENAO received Ph.D. degree in Engineering from Pereira Technological University, Pereira, Colombia, in 2021. Now he works at Pereira Technological University. His current research interests include mechanisms analysis, Internal combustion machine, and machine design.